STUDIECENTRUM VOOR KERNENERGIE

CENTRE D'ETUDE DE L'ENERGIE NUCLEAIRE

# THE USE OF THE JEM 1250 HIGH VOLTAGE ELECTRON MICROSCOPE (HVEM) OF THE UNIVERSITY OF ANTWERP (RUCA) AS AN INSTRUMENT FOR VOID SWELLING SIMULATION EXPERIMENTS

M. SNYKERS, C. JANSSENS

January 1978

BLG 521

144, avenue E. Plasky, BRUXELLES 4
(BELGIQUE)

E. Plaskylaan 144, BRUSSEL 4
(BELGIE)

M. SNYKERS, C. JANSSENS
BLG 521 (Jan. 1978)

THE USE OF THE JEM 1250 HIGH VOLTAGE ELECTRON MICROSCOPE (HVEM) OF THE UNIVERSITY OF ANTWERP (RUCA) AS AN INSTRUMENT FOR VOID SWELLING SIMULATION EXPERIMENTS

Summary. - The working procedure has been established for the use of the high voltage electron microscope of the University of Antwerp (RUCA) as an apparatus for testing the swelling behaviour of ferritic and austenitic stainless steels. The local temperature increase of the specimen due to beam heating was measured. The results are in good agreement with measurements done in other laboratories. The intensity of the transmitted beam has been measured as a function of specimen thickness (for thicknesses smaller than a few μm). The operation conditions are described for carrying out irradiation experiments and for taking stereo pairs.

M. SNYKERS, C. JANSSENS
BLG 521 (Jan. 1978)

THE USE OF THE JEM 1250 HIGH VOLTAGE ELECTRON MICROSCOPE (HVEM) OF THE UNIVERSITY OF ANTWERP (RUCA) AS AN INSTRUMENT FOR VOID SWELLING SIMULATION EXPERIMENTS

Samenvatting. - De werkingsmetode om de hoogspannings-elektronenmikroskoop van de universiteit van Antwerpen (RUCA) te gebruiken om het zwelgedrag van roestvaste austeniet- en ferrietstalen te testen onder invloed van elektronenbestraling werd op punt gezet. De lokale temperatuurstijging van het specimen onder invloed van de elektronenbundel werd gemeten, de resultaten zijn in goede overeenstemming met metingen gedaan met andere elektronenmikroskopen. De intensiteit van de doorgelaten bundel als funktie van de dikte van het specimen werd gemeten voor kleine dikten van het specimen (tot enkele μm). De werkingsvoorwaarden worden beschreven voor het uitvoeren van bestralingen en het nemen van stereoparen.

M. SNYKERS, C. JANSSENS
BLG 521 (Jan. 1978)

THE USE OF THE JEM 1250 HIGH VOLTAGE ELECTRON MICROSCOPE (HVEM) OF THE UNIVERSITY OF ANTWERP (RUCA) AS AN INSTRUMENT FOR VOID SWELLING SIMULATION EXPERIMENTS

Résumé. - Les conditions d'opération du microscope à haute tension de l'université d'Anvers (RUCA), comme appareil pour étudier le gonflement d'aciers austénitique et ferritique, ont été mises au point. L'augmentation de la température locale sous l'influence du faisceau électronique a été mesurée; les résultats sont en bon accord avec les mesures faites par d'autres microscopes. L'intensité du faisceau transmis en fonction de l'épaisseur de l'échantillon a été mesurée pour des faibles épaisseurs (jusqu'à quelques μm). Les conditions de travail pour effectuer des irradiations ainsi que pour prendre des photos stéréoscopiques sont décrites.

# THE USE OF THE JEM 1250 HIGH VOLTAGE ELECTRON MICROSCOPE (HVEM) OF THE UNIVERSITY OF ANTWERP (RUCA) AS AN INSTRUMENT FOR VOID SWELLING SIMULATION EXPERIMENTS

M. SNYKERS, C. JANSSENS

January 1978

BLG 521

This report has been written in collaboration with Prof. J. VAN LANDUYT from the "Centrum voor HSEM" - RUCA Antwerp and Dr P. DELAVIGNETTE from the S.C.K./C.E.N. MOL.

## 1. INTRODUCTION

After the discovery of void swelling in nuclear reactor structural materials by CAWTHORNE and FULTON (1966) several void swelling simulation techniques have been developed. The two main types make use of either energetic ions or energetic electrons. Their main advantage is that the swelling rate may be increased by two to three orders of magnitude compared with reactor irradiations.

Energetic heavy ions create the same kind of defects as neutron damage i.e. the cascade type. However in this case the vacancies tend to form vacancy loops which lowers the excess of free vacancies versus interstitials which is necessary for swelling in a reactor. These vacancy loops can anneal thermally at temperatures higher than 350° C. In ion simulation experiments where the defect production rate is increased by two to three orders of magnitude the temperature where these vacancy loops anneal is considerably higher. Generally, the ion simulation experiments only give accurate swelling simulation information at temperatures near the peak swelling temperature.

Energetic electrons (1 MeV) create mainly single Frenkel pairs. They do not give rise to the formation of vacancy loops. Therefore swelling can be observed at very low temperatures by means of HVEM. Simulation by means of HVEM may give accurate information of the actual swelling rate at all temperatures.

The actual swelling data obtained by means of the different techniques are not immediately comparable because of the differences in the threshold swelling dose. A good agreement is obtained between the HVEM results and the in-reactor swelling results if one compares the swelling rates. The same is true for ion simulation results obtained at the peak swelling temperature.

The products of transmutation reactions in a reactor cannot be adequately simulated in a HVEM experiment. These products which have a marked influence on the swelling results may be pre-injected in the specimen. This means that during the HVEM swelling experiment the ratio of the dpa to transmutation product concentration is not correct, which may influence the results.

The advantage of swelling experiments by means of a HVEM is that the whole swelling process can be observed in situ. Pioneering work on the latter has been carried out by MAKIN in Harwell (1971). The main problems in simulation experiments by means of a HVEM are the following :

- the control and determination of the local specimen temperature ;
- the determination of the local beam intensity ;
- the calculation of the number of displacements per atom (dpa) ;
- the determination of the local specimen thickness and the void layer thickness ;
- the rôle played by the foil surfaces.

The HVEM is an excellent tool for studying the mechanism of swelling and, in most cases, gives a good indication of the degree of resistance against swelling of different materials. A lot of work still has to be done before its actual swelling results may be used for a reactor design.

The work that will be described next has been performed in the framework of the ferritic steel programme, and therefore most of the attention will be focused on ferritic alloys.

## 2. BEAM INTENSITY AND BEAM PROFILE

The JEM 1250 microscope is schematically shown in Fig. 1. It is equipped with two Faraday cages, one at the level of the specimen and one after the projector lens. With these two cages it is possible to measure the eventual loss of current in the magnifying part of the microscope (between specimen and photographic screen). With a fully focused beam there is no measurable loss of current. This means that the current intensities measured with the lower Faraday cage give the exact value of the current received by the specimen.

There are three possible settings of the condensor 1 lens which result in three minimum spot sizes of about 4, 10 and 20 µm. The beam profiles have been measured for the three settings by means of the lower Faraday cage. The diameter of the hole in the Faraday cage is 4 mm. At the specimen level this corresponds to a diameter of $\frac{14.46}{M}$ mm (if M is the magnification at the photographic plate level). The relation between the current density measured with the Faraday cage and the current density

at the specimen level is

$$I_{sp} = \frac{I_{FC} \times M^2}{1.6} \ (A/cm^2)$$

where $I_{sp}$ = local current density at specimen level ;
$I_{FC}$ = current density at the Faraday cage level.

The beam profile is determined by varying the magnification. Some beam profiles are shown in Fig. 2. If the microscope is correctly aligned, the beam profile is symmetrical about the beam axis and can be represented by the Gaussian relation.

$$I\ (r) = I_o \exp. \quad 0.7\ (\frac{r}{a})^2$$

when r = distance from the beam axis ;
a = the half width at half maximum of the peak ;
$I_o$ = peak intensity.

The beam diameters at specimen level, which contain about 90 % of the total beam current are 2, 4 and 8 µm respectively. The maximum total beam currents are 0.3, 0.7 and 1.5 µA respectively. The conditions obtained with the second spot size are quite close to those given by the AEI HVEM in Harwell, which favours comparison of results.

## 3. LOCAL SPECIMEN TEMPERATURE

The specimen temperature is set by means of a small oven in the top of the side entry specimen holder. A temperature increase due to beam heating has to be taken into account. The actual temperature of the irradiated area is

$$T_{loc} = T_{oven} + \Delta T_{beam}$$

The temperature of the oven $T_{oven}$ is measured by means of a thermocouple, spot-welded on the oven. The temperature increase due to beam heating $\Delta T_{beam}$ is very difficult to measure. Techniques based on eutectic transformations or melting of a phase with a low melting point are only relevant, if its thermophysical properties are comparable with those of the specimen to be irradiated (in our case ferritic alloys with composition about Fe 13 Cr 2 Mo 2 Ti). Since we did not find such a material we intended to use a method introduced by MAKIN (1971). He makes use of the property that the mean void diameter for swelling of AISI 316 SS is a strong and nearly linear function of temperature between 400 and 600° C. If the mean void diameter is determined as a function of temperature with two different total beam cur-

rents $I_1$ and $I_2$, but the same central beam current, then the actual temperatures for the tests are $T + \Delta T_1$ and $T + \Delta T_2$ respectively where T is the temperature measured with the oven and $\Delta T_1$ and $\Delta T_2$ are proportional to $I_1$ and $I_2$ respectively. The temperature increase due to beam heating results from $\Delta T_2 - \Delta T_1 \propto I_2 - I_1$.

This is an interesting method for materials which have high swelling rates as is the case for AISI 316. For materials with a low swelling rate like the ferritic alloys, this method becomes very inaccurate. However, if the thermophysical properties of the AISI 316 and of the ferritic alloy are comparable, the first one may be used for the temperature calibration of ferritic alloys.

Therefore some preliminary tests were carried out in order to compare their thermophysical properties.

In a first series of tests,the temperature increase due to beam heating measured with the thermocouple of the oven was evaluated for AISI 316 SS and a ferritic alloy $S_4$ (Fe 13 Cr 0.8 Mo 0.2 Ti) as a function of

- the total beam current ;
- the thickness of the irradiated area ;
- the initial temperature of the oven.

The temperature increase of the oven was measured as a function of the actual transmitted intensity (I), measured with the Faraday cage at a standard magnification of 15,000 and without the condensor 2, the objective and the selected area diaphragms. The results are shown in Fig. 3 and Fig. 4. For relatively small thicknesses the increase is roughly proportional to $I_T/I_o$ and for the same thickness the increase is proportional to the initial beam intensity.

No temperature increase was measured with the thermocouple of the oven for thicknesses which were of interest in swelling experiments. A comparison between the results obtained with the oven temperature set at room temperature and 400° C shows that, at 400° C, the temperature increase is much less than the increase obtained at room temperature. This is due to increased radiation losses at 400° C and a decrease in the thermal conductivity of the specimen. The results obtained on AISI 316 SS and on the ferritic alloy $S_4$ are identical in these respects. This enables us to use AISI 316 SS for further temperature calibration.

We have repeated Makin's experiment in slightly different conditions. The mean void

diameter is determined for two different temperatures and two different total and local beam currents. The fact that we use different local beam currents gives a slight underestimation of the actual temperature increase. The results are shown in Fig. 5. The relative shift of the two graphs gives the temperature increase of the specimen due to the difference in the two total beam currents ($I_2 - I_1$). Keeping in mind that $\Delta t \propto I$ we found that the local temperature increase is between 4 and 8° C per 0.1 µA of total beam current. This agrees well with the results obtained by MAKIN. These values do not fit in so well with the computation done by FISHER (1970). For iron at room temperature and for beam and specimen conditions about the same as the conditions in our experiment he finds a temperature increase higher than 40° C. At 400° C this difference should still be higher due to the change in thermal conductivity. These results from Fisher's calculations may be considered as upper limits of temperature increase because they are carried out for foils with constant thickness, while the specimens are in fact wedge-shaped, which is more favourable for the thermal conduction.

The local temperature increase obtained here is only valid for materials with thermophysical properties similar to AISI 316 SS in the temperature range of interest. For other materials a new calibration has to be carried out.

## 4. THICKNESS OF THE IRRADIATED AREA AND OF THE VOID LAYER

The choice of an adequate thickness is essential for significant swelling simulation in HVEM. Specimens which are too thin will not allow a simulation of the bulk material due to surface effects. On the other hand, specimens which are too thick cause overlapping of the voids. The foil thickness may be determined by means of the change in the projected width of a planar defect such as a grain boundary.

This is used for the calibration of the decrease in transmitted beam intensity as a function of specimen thickness.

The beam intensity was measured using the second objective aperture. If all objective apertures are out, the sensitivity of the decrease in transmitted beam intensity as a function of specimen thickness is too low for the thickness of interest. All measurements must be taken in kinematical beam conditions in order to obtain reliable measurements. The results are shown in Fig. 6. The specimen thickness measured in this way is only important for setting the initial experimental conditions. For swelling evaluations the void layer thickness is of prime interest. This thickness is different from the specimen thickness due to surface effects.

Furthermore, the thickness of the denuded zones is a function of the temperature and the material. The thickness of the void layer is determined by means of stereographic observations. These observations must be made in kinematical conditions because in dynamic conditions the dislocation contrast renders the voids invisible. This is a serious problem because due to swelling the specimen is locally deformed which makes it difficult to get rid of bend contours.

The void layer thickness may be calculated from stereographic observations by means of the expression (see also Fig. 7)

$$d = \frac{P}{2\,M \sin \alpha/2}$$

where $P$ = parallax ;

$M$ = magnification of the micrographs ;

$\alpha$ = angle between the stereopair.

## 5. PRACTICAL GUIDELINES

The JEM 1250 microscope is equipped with a liquid nitrogen cold trap in the vacuum system. With this cold trap a vacuum of $5 \times 10^{-7}$ torr may be reached in the column. This is very useful for irradiation tests in the temperature range from 400-700° C. It has been noticed that with a vacuum of $5 \times 10^{-6}$ torr, specimens of AISI 316 SS oxidized at 550° C and specimens of ferritic alloys at 460° C.

It is therefore advised that the cold trap should be used during irradiation experiments at a high temperature.

Bad alignment of the filament and accelerater column gives a non-circular fully-focused beam. This has to be avoided because of the increase in the total beam intensity versus the maximum central intensity which gives an unnecessary increase of the temperature of the specimen, and increases the temperature error.

Irradiations should be carried out with the condensor 2, objective and selected area apertures out. The fixed aperture in the C2 condensor lens enables us to obtain a beam profile which is comparable with other types of microscopes like the AEI in Harwell. The objective diaphragm has to be out because this gives additional heating due to irradiation from the diaphragm.

A guideline list is given in Table 1.

## 6. THE NUMBER OF DISPLACEMENTS PER ATOM

It is not the aim of this paper to give a detailed account of the calculations yielding the number of displacements per atom. There are several detailed review papers relative to this subject (ETHERINGTON et al., (1973) OEN, (1965, 1973) DORAN (1976)).

Only a short survey will be given.

An electron impinging on a solid has a certain atomic collision probability and may transfer energy to the solid. The maximum transferable energy is given by :

$$E_m = 2\,E\,\frac{E + 2\,mc^2}{Mc^2}$$

where m = mass of electron ;
M = mass of target atom ;
E = energy of electron.

The energy transferred depends on the collision angle. Only those atoms which receive an energy quantity

$$E > E_d$$

will be displaced where $E_d$ = atomic displacement threshold energy.

The number of displaced atoms (primary knock on atoms PKA) is given by :

$$N_P = \emptyset \cdot \sigma_P$$

where $\emptyset$ = electron flux ;
$\sigma_P$ = displacement cross-section giving the number of PKA produced per matrix atom by an incident fluence of 1 particle/cm$^2$.

For the displacement cross-section the values calculated by OEN (1965) (1973) are generally used. There still exist uncertainties about the displacement energy threshold for several materials. This means that $\sigma$ cannot be calculated correctly for these materials.

The number of displaced atoms may be increased due to secondary displacements if the energy of the PKA is higher than 2 $E_d$. For 1 MeV electrons impinging on an iron base alloy this increase is rather low and therefore it is generally accepted that the total number of displaced atoms N is equal to the number of PKA. The different

models giving an estimate of the number of dpa are :

1. The Kinchin-Pease model.

2. The half-Nelson model.

3. The NRT model (S).

The "NRT standard" is most currently used nowadays. For iron base alloys a displacement threshold of 40 eV is used for the calculation. The number of displaced atoms of an iron base alloy is :

$$N = N_P = \emptyset \cdot \sigma (E_d = 40 \text{ eV}).$$

## 6. EVALUATION OF THE SWELLING DATA

In the initial stages of irradiation the dislocation density rapidly increases up to a level where the measurement of their density becomes very difficult. Therefore the evaluation of the dislocation density is only of interest for very low doses (<< 1 dpa). For the reactor technologist the actual void swelling is more important. In order to evaluate the void data, the micrographs are magnified to a standard magnification. Histograms are made of the void size distribution for a standard area (e.g. by means of the Zeiss particle size analyser available at R.U.C.A.). This gives the mean void diameter and the diameter of the mean void volume $\bar{d}_v$ . As we are interested in actual swelling, the latter is more important.

It can be calculated as follows.

$$\bar{d}_v = \left(\frac{1}{N} \sum_{i=o}^{N} d_i^3\right)^{1/3}$$

where N is the total number of voids considered in a certain volume V and $d_i$ is a measured void diameter.

The main void volume is

$$\bar{v} = \frac{1}{6} \pi \bar{d}_v^3$$

The void swelling is then given by

$$S = \frac{\Delta V}{V - \Delta V} = \frac{N \cdot \bar{v}}{V - N \cdot \bar{v}}$$

## 7. SOURCES OF ERROR

There are several possible sources of error. The first one is due to beam intensity variations during the experiment. The beam intensity may drop by 5 to 10 % within the first hour of operation. Therefore it is necessary to measure the intensity before and after the experiment.

The absolute error due to magnification is of the order of 10 %, but since mainly comparative measurements are performed, and if care is taken to position the specimen with the available height control provision and the appropriate photographic paper for enlargements is used, this error is negligible. The main sources of error are due to incorrect measurements of the void layer thickness and the void size distribution. Therefore it is important to choose the area with the appropriate thickness. It is difficult to give a correct estimate of the magnitude of the error because it depends on the particular experimental conditions. However, generally it will be at least of the order of 20 %.

# REFERENCES

1. C. CAWTHORNE and E.J. FULTON
Nature, 216, 575 (1966).

2. M.J. MAKIN
A.E.R.E. R 6957 (1971).

3. S.B. FISHER
Radiation Effects 5, 239 (1970).

4. E.W. ETHERINGTON et all.
A.E.R.E. R 7374 (1973).

5. O.S. OEN
O.R.N.L. 3813 (1965),
O.R.N.L. 4897 (1973).

6. D.G. DORAN et all.
H.E.D.L.-S.A. 1058,
H.E.D.L.-T.M.E. 73-76.

## TABLE 1

### Practical guidelines for void swelling experiments

1. Vacuum : Liquid $N_2$ cold trap on column vacuum meter $10^{-6}$ range (for automatic shut-off).

2. Beam : Circular fully focused.
   Measuring the intensity at magnification of 1000 and 15000.

3. Specimen thickness : Initial measurement.
   Condensor 2 diaphragm out.
   Obj. diaphragm 2 in.
   Look for an area where $3 < I_T/I_0 < 5$ in kinematical beam conditions ; the value to be selected depends on the material and the temperature.

4. Irradiations : All movable diaphragms out.

5. Micrographs : Taken in kinematical beam conditions.

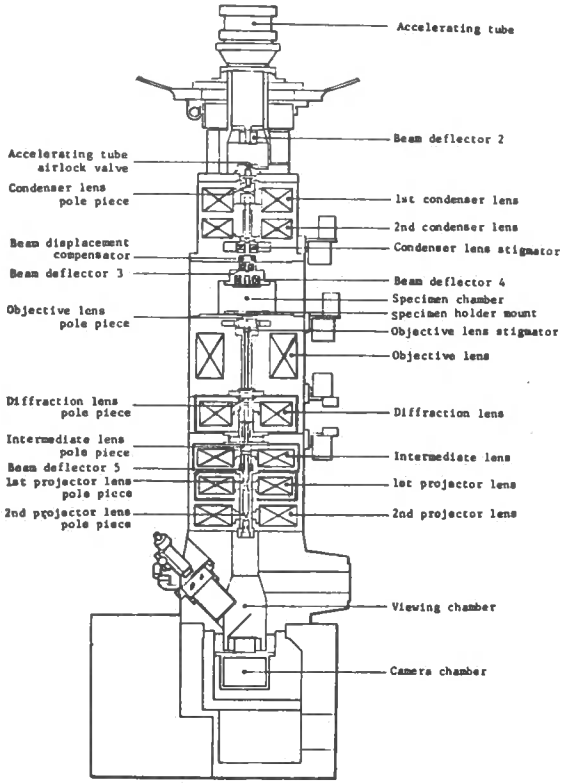


Cross-sectional view of the JEM-1250 (2/2)

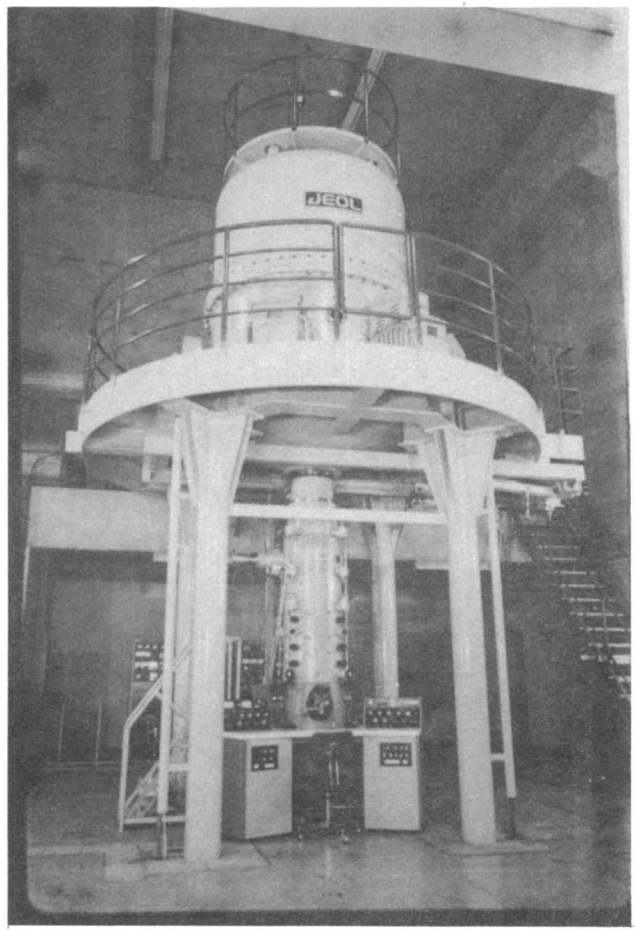


FIG. 1.

The JEM 1250 electron microscope.

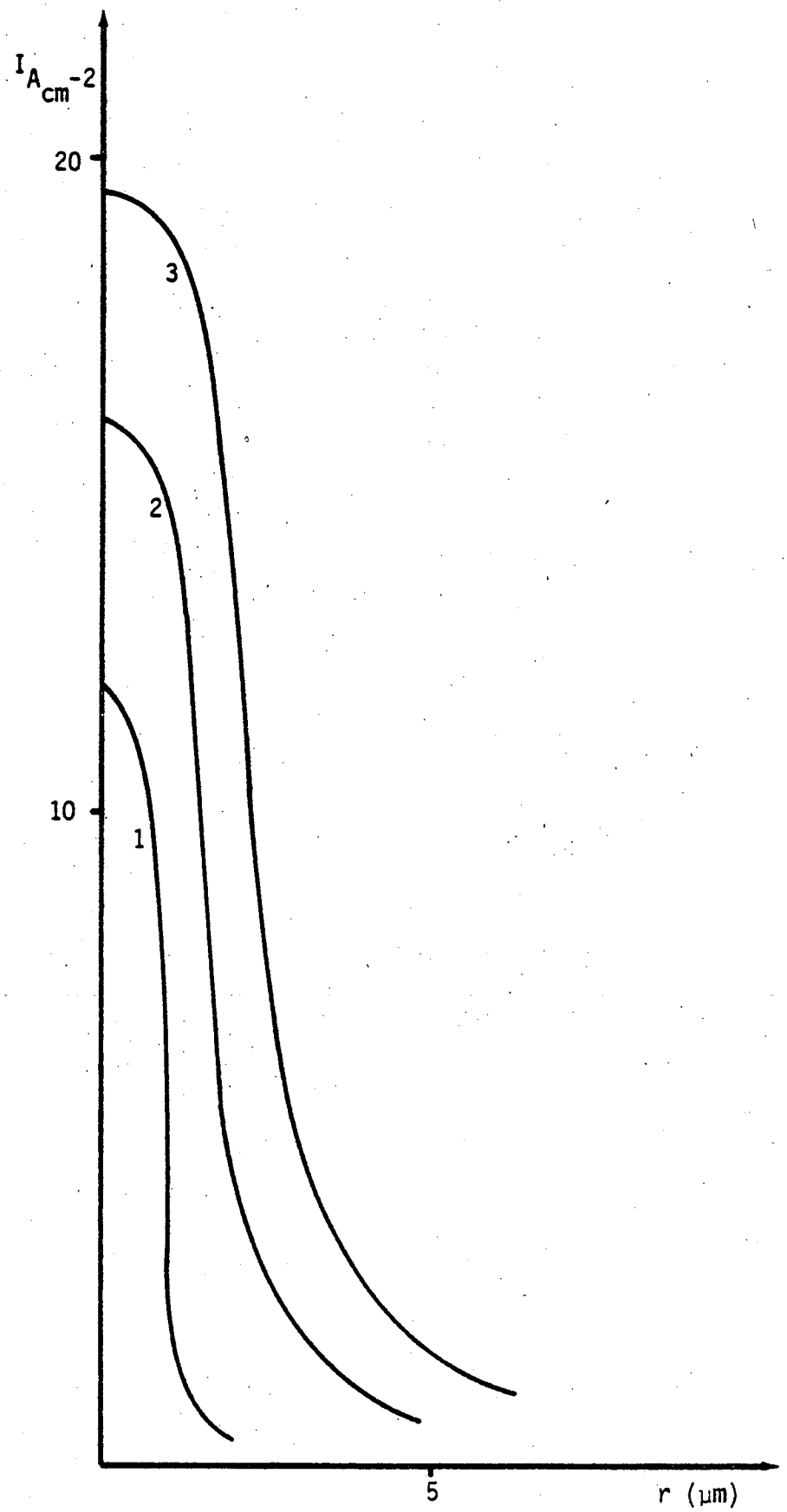


FIG. 2.

Beam profiles for spot size 1,2 and 3.

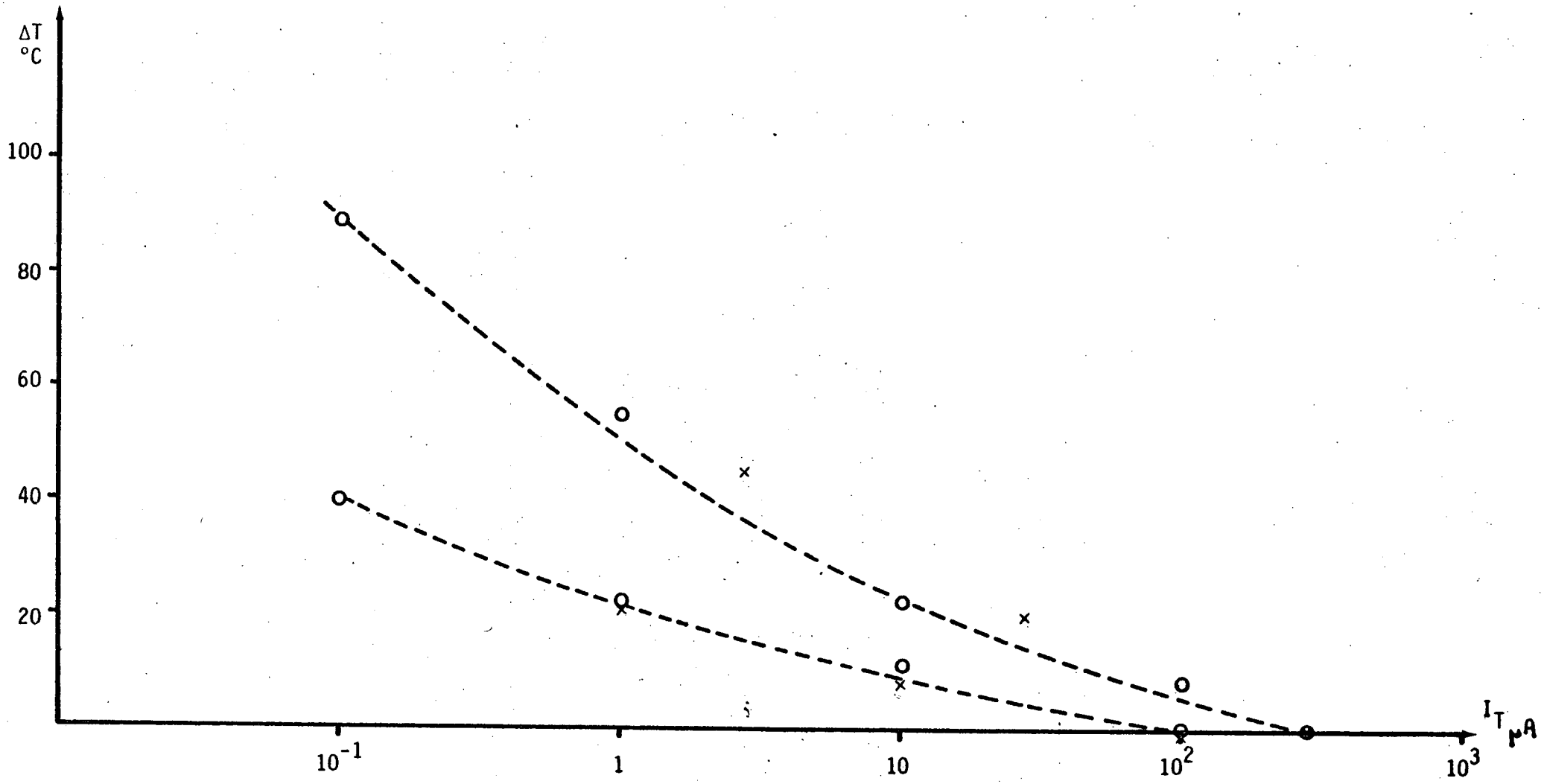


FIG. 3.

Temperature rise of the specimens AISI 316 (O) and $S_4$ (X) as a function of the transmitted intensity ($I_T$) measured at room temperature with the thermocouple of the oven.

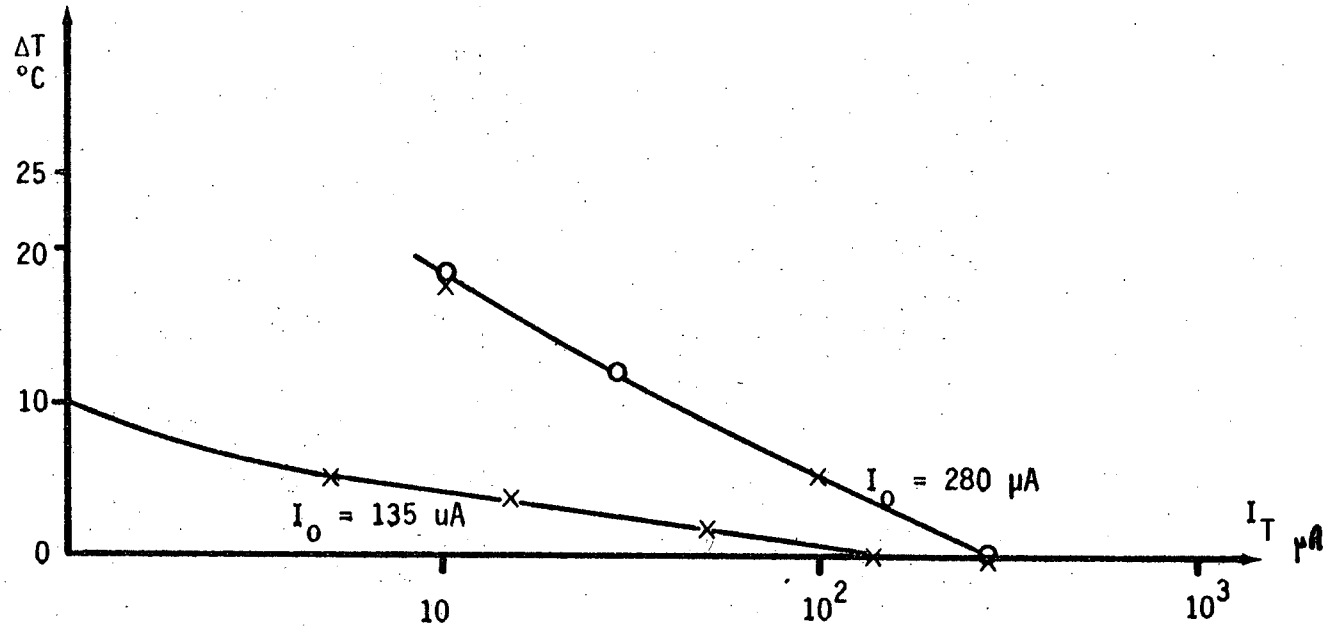


FIG. 4.

Temperature rise of the specimens AISI 316 (O) and $S_4$ (X) as a function of the transmitted intensity ($I_T$) measured at 400°C with the thermocouple of the oven.

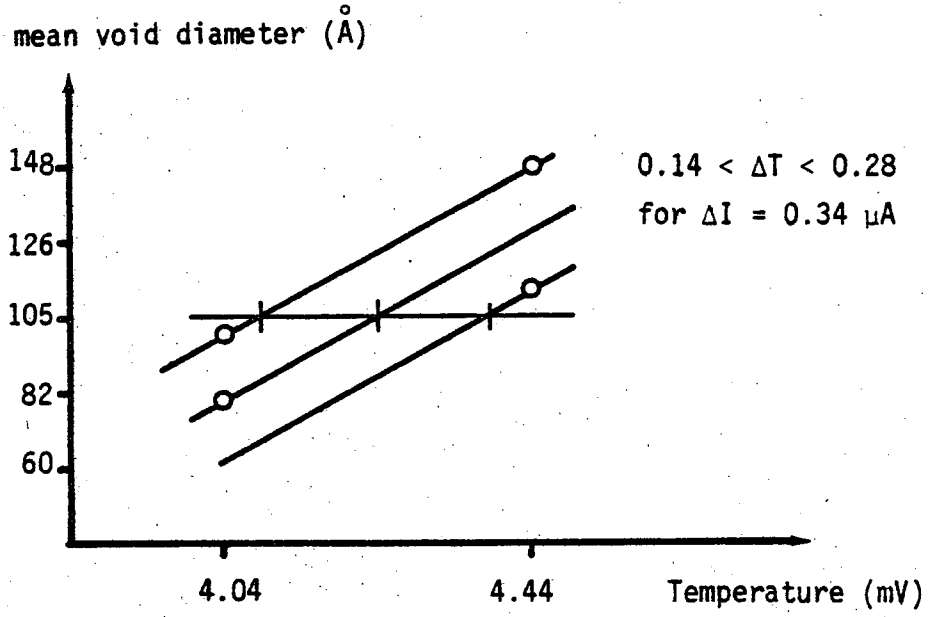


FIG. 5.

Mean void diameter as a function of temperature for two different total beam intensities.

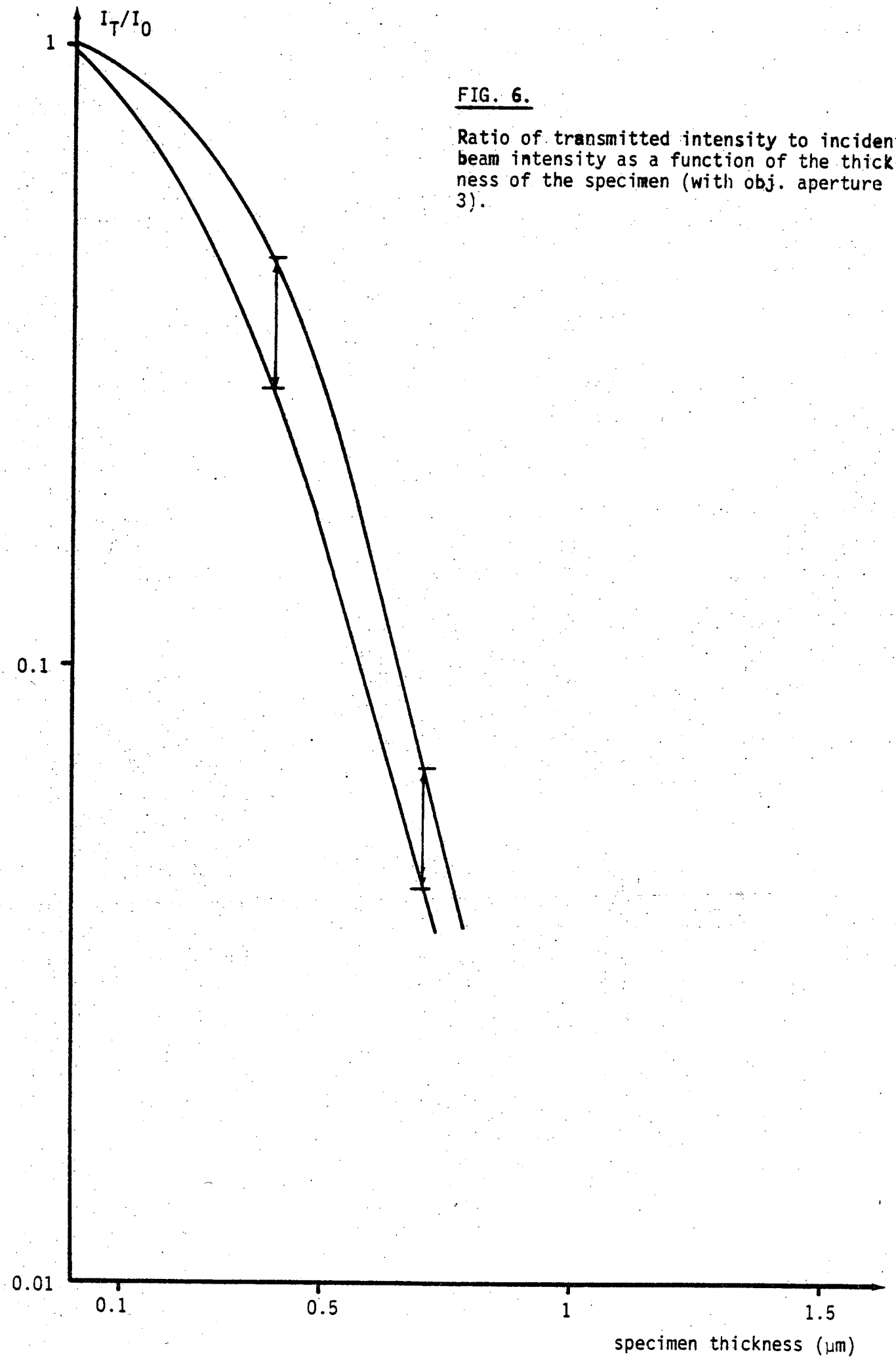


FIG. 6.

Ratio of transmitted intensity to incident beam intensity as a function of the thickness of the specimen (with obj. aperture 3).

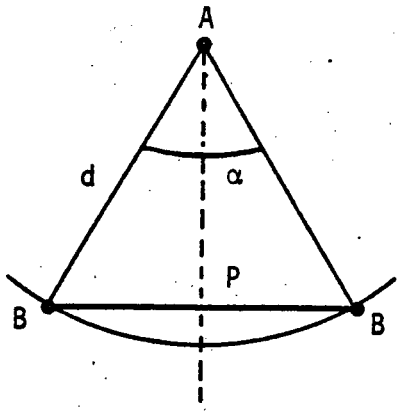


FIG. 7.

Schematic representation of the geometric situation of stereographic pictures taken under an angle α from the objects A and B with a depth difference d. This gives rise to a parallax P.

X